

## CHAPTER 3

# Peptide-Functionalized Quantum Dots for Live Diagnostic Imaging and Therapeutic Applications

Laurent A. Bentolila, Sören Doose, Yuval Ebenstein, Gopal Iyer, J. Jack Li, Xavier Michalet, Fabien Pinaud, James Tsay and Shimon Weiss

### 3.1 Introduction

Since their first appearance as optical probes in biological imaging [1, 2], qdots have been applied in most biotechnological applications using fluorescence, including DNA array technology, immunofluorescence assays (reviewed in [3]), and cell and animal biology (reviewed in [4, 5]). Qdots have gained wide acceptance by the scientific community and the biotechnology industry as new fluorescent, nonisotopic labels of unmatched potentials. Most appealing to the biosciences are the high brightness, high resistance to photobleaching, and the ability to size-tune fluorescent emission of these inorganic-biological hybrid nanostructures. Qdots have also proved to be excellent probes for two-photon confocal microscopy and deep-tissue imaging given their large two-photon absorption cross-section [6–9]. But it is when combined with ultrasensitive microscopy techniques that qdots have shown their true potential by allowing visualization of cellular processes down to the molecular scale [10–13]. The enhanced photophysical properties of qdots can fulfill the stringent requirements needed to provide spatial, temporal, and structural information at all length scales: from the whole body down to the nanometer resolution with a single probe.

Fluorescent nanocrystals of semiconductor material, which are generally synthesized in solutions of nonpolar organic solvents using colloidal chemistry [14], require additional chemical modifications to be solubilized in aqueous buffers and functionalized for biological applications (see Chapter 1, “Colloidal Quantum Dots: Synthesis, Photophysical Properties, and Biofunctionalization Strategies,” by Susumu et al. for an in-depth discussion). This can be achieved by either surfactant exchange, a process primarily driven by mass-action in which the native TOP/TOPO hydrophobic surface ligands are substituted with bifunctional amphiphilic ones, or by insulation of the original hydrophobic qdot within a heterofunctional amphiphilic coating [4, 5]. These various qdot solubilization strategies have included the following: (1) ligand exchange with small thiol-containing

molecules [2, 15] or more complex ones such as oligomeric phosphines [16], dendrons [17], and peptides [18, 19]; (2) encapsulation by a layer of amphiphilic diblock [20], or triblock copolymers [21], in silica shells [1, 22], phospholipid micelles [23], polymer beads [24], polymer shells [25], or amphiphilic polysaccharides [26]; and (3) combination of layers of different molecules conferring the required colloidal stability to qdots [27, 28]. Once the qdots have been solubilized with hydrophilic ligands, those can serve as anchoring points for the chemical attachment of biomolecules to functionalize the qdot's surface. Qdot's ligands containing either an amine or a carboxyl group offer the possibility to crosslink molecules containing a thiol group [18, 23, 29] or an N-hydroxysuccinimyl-ester moiety [1, 19] using standard bioconjugation reactions.

Another approach uses electrostatic interactions between qdots and charged molecules, or proteins modified to incorporate charged domains [30]. These functionalization steps can be repeated to add or change functionality. For instance, streptavidin-coated qdots can be used in combination with biotinylated proteins, antibodies, or nucleic acids [10, 19, 20, 31–34]. By extension, a generic three-layer approach using (1) an antibody against a specific target, (2) a biotinylated secondary antibody against the first, and (3) a streptavidin-coated qdot allows qdot labeling of most types of targets [10, 20]. However, the “sandwich” approach results in large structures that may impede further use of qdots in some applications. This issue can be minimized by using small peptide derivatives for qdot solubilization and/or functionalization. The utility of peptides in qdot chemistry stems from several characteristics. Thiol-containing peptide sequences (i.e., Cysteine) have the capacity to coordinate with the nanocrystal shell surface after ligand exchange of the TOPO coating. This leads to a direct attachment of the peptide to the qdot. While small, peptides still maintain excellent molecular recognition properties that allow them to participate in ligand-receptor and protein-protein molecular interaction with high affinity. For example, it has been shown that a ~30 amino acids peptide hairpin against Texas Red has a dissociation constant  $K_d$  of ~25 pM [35]. Peptides provide selective anchor points for independent chemical modifications. They offer flexible platforms to screen vast combinatorial libraries with the aim of mutating the peptide sequences to optimize the colloidal and photo-physical properties of nano-materials [36, 37]. Finally, peptides are usually easy to synthesize or mass produce in recombinant hosts.

Our laboratory and others have harnessed these properties to develop unique peptide-based solubilization, functionalization, and targeting approaches that maintain the overall size of the qdot bioconjugate as relatively small while yielding monodisperse water-soluble qdots that remain bright and photostable. In the “conventional” two-step approach, solubilization and functionalization are usually uncoupled. Qdots are first solubilized through one of the many approaches described previously before a functional peptide sequence could be attached to the qdots' surface through covalent conjugations or self-assembly. (For a review, see [38].) We will refer to these probes as “peptide-conjugated” qdots. On the other hand, our laboratory has developed a single-step solubilization/functionalization approach based on exchanging the qdots' surface ligands with bi-functional amphiphilic peptides [19]. In the rest of this chapter, we will refer to this approach as *peptide coating*. The peptide-coating approach has been successful on several

types of core and core-shell qdots encompassing the visible to the near-infrared (NIR) spectral range. In this chapter, we first describe the peptide-coating approach and briefly assess the colloidal and photophysical properties of the resulting peptide-coated particles when tested by fluorescence correlation spectroscopy (FCS) and single-molecule spectroscopy (SMS). We then continue with several examples of biological applications in which peptide-coated qdots have been used. Those include single-particle tracking of membrane receptor in live cells and combined fluorescence and micro-positron emission tomography ( $\mu$ PET) imaging of targeted delivery in live animals. Beyond diagnostic imaging, they also have shown utility in other sensing and therapeutic applications including the development of novel protease assays and the use of photo-induced cellular targeted killing. We finally conclude with a brief overview of future developments.

### 3.2 Phytochelatin Peptides: The All-in-One Solubilization/ Functionalization Approach

The use of semiconductor qdots for biological applications requires that they are water soluble and offer reactive chemical groups on their surface for the subsequent conjugation of molecules and compounds of biological interest. In contrast to the more conventional multiligand/multilayer approaches mentioned previously, our group has developed a new peptide-based family of ligands that replaces the shell surface TOPO coating and fulfills all the stringent requirements of a biocompatible imaging probe at the same time. These engineered peptides maintain most of the original qdot photophysical properties, solubilize qdots in aqueous buffers, provide a biological interface to the qdot, and allow multiple functions to be easily incorporated all in a single easy step. This surface chemistry was designed to be simple, robust, amenable to high-throughput molecular evolution, and flexible enough to suit the different needs of the experimentalists. This is achieved by exchanging the surfactants with synthetic phytochelatin-like  $\alpha$ -peptides [19].

Phytochelatin is a glutathione-related, cysteine-rich isopeptide synthesized by some plants, yeast, and bacteria strains to detoxify their environment from heavy metal ion contaminants (i.e.,  $\text{Cd}^{2+}$  [39]) by inducing their nucleation into semiconductor qdots particles (i.e.,  $\text{CdS}$  [40, 41]). These peptides of general structure  $(\text{Glu-Cys})_n\text{Gly}$  (designed  $(\gamma\text{-EC})_n\text{G}$  or  $(\alpha\text{-EC})_n\text{G}$  depending on the peptide linkage between the glutamate and cysteine residues) follow a strict periodicity (with  $n$  being the number of di-peptide repeats typically ranging from 2 to 4), which acts as a template for the nucleation and intracellular growth of the qdots (Figure 3.1). Interestingly, the resulting peptide-coated qdots grown *in vivo* show similar photo-luminescent properties when compared to the chemically synthesized ones, with the only notable exception of being less stable and more prone to degradation upon photo-excitation [41]. One possible reason is their lower crystalline quality, but it also may be due to the absence of higher band gap shell material grown on top of the semiconductor cores. For this reason, qdots grown from natural peptide templates have found very little use as probes for biological imaging.

The phytochelatin-like  $\alpha$ -peptides developed in our laboratory have been inspired by these naturally occurring processes. Such synthetic sequences efficiently

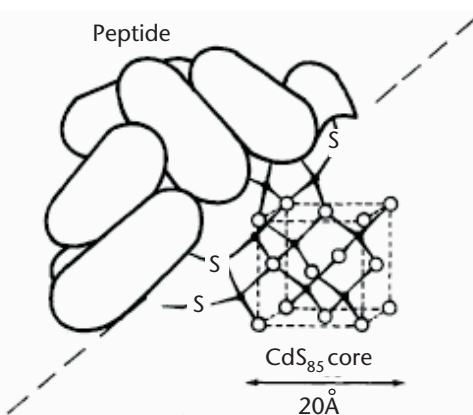


**Figure 3.1** Hypothetical model structure of a natural phytochelatin peptide-coated CdS crystallite from yeast. The cysteinyl thiolates of approximately 30 ( $\gamma$ -EC)<sub>n</sub>G peptides are surface ligands to the core of about 85 CdS units. The yeast qdots are monodisperse with an average diameter of 20Å. Adapted from [41] with permission from Elsevier.

bind to the surface of ZnS capped CdSe qdots synthesized *in vitro* in the presence of TOPO surfactant. A typical amphiphilic peptide is about 20 amino acids long (Figure 3.2(a) and Table 3.1). It is composed of two distinct domains: a metal-chelating adhesive domain containing multiple cysteines (Cys) and unnatural hydrophobic amino acids 3-cyclohexylalanines (Cha), and a negatively charged hydrophilic tail domain. The hydrophobic domain is primarily responsible for the recognition and attachment to the qdot shell surface, while the hydrophilic one ensures solubilization and stability in buffers. The sequence composition of the metal-binding domain is fixed, and the spacing of the cysteinyl thiolates ensures proper anchorage on CdS and ZnS qdot's surfaces [41–43]. We have found that substituting the Cys residues by alanine (Ala) resulted in water insoluble particles, thus confirming the essential role of the Cys in binding of the peptides onto the qdot's surface. We also observed that a single adhesive domain repeat resulted in unstable qdots. We thus opted for multiple tandem repeats of Cys, which enhanced the stability of the peptide on the qdots most likely by providing better surface coverage. A similar length-dependent stability was previously reported for CdS qdots coated with phytochelatin peptides of various lengths [41]. The presence of the Cha residues around the Cys in the adhesive domain helps the solubilization of the peptides in an 9:1 (v:v) pyridine:dimethylsulfoxide (DMSO) cosolvent mixture where TOPO-coated qdots are stable, therefore limiting the formation of aggregate during the reaction. The large cyclohexyl moieties were also chosen to limit the cross-reactivity between the Cys of the adhesive domain and to compete with the hydrophobic TOPO on the qdot's surface. When the Cha residues were replaced by Ala, the peptide-coated qdots we obtained were unstable in buffers. However, we have been recently successful in replacing the unnatural amino-acid Cha by a natural one, phenylalanine (Phe), in the metal-binding domain that still preserves the stability and photophysical properties of the peptide-coated qdots [44]. One direct advantage of this substitution is that an “all natural” peptide (peptide 8 in Table 3.1) can be mass-produced in bacteria. This represents a cost-effective alternative to

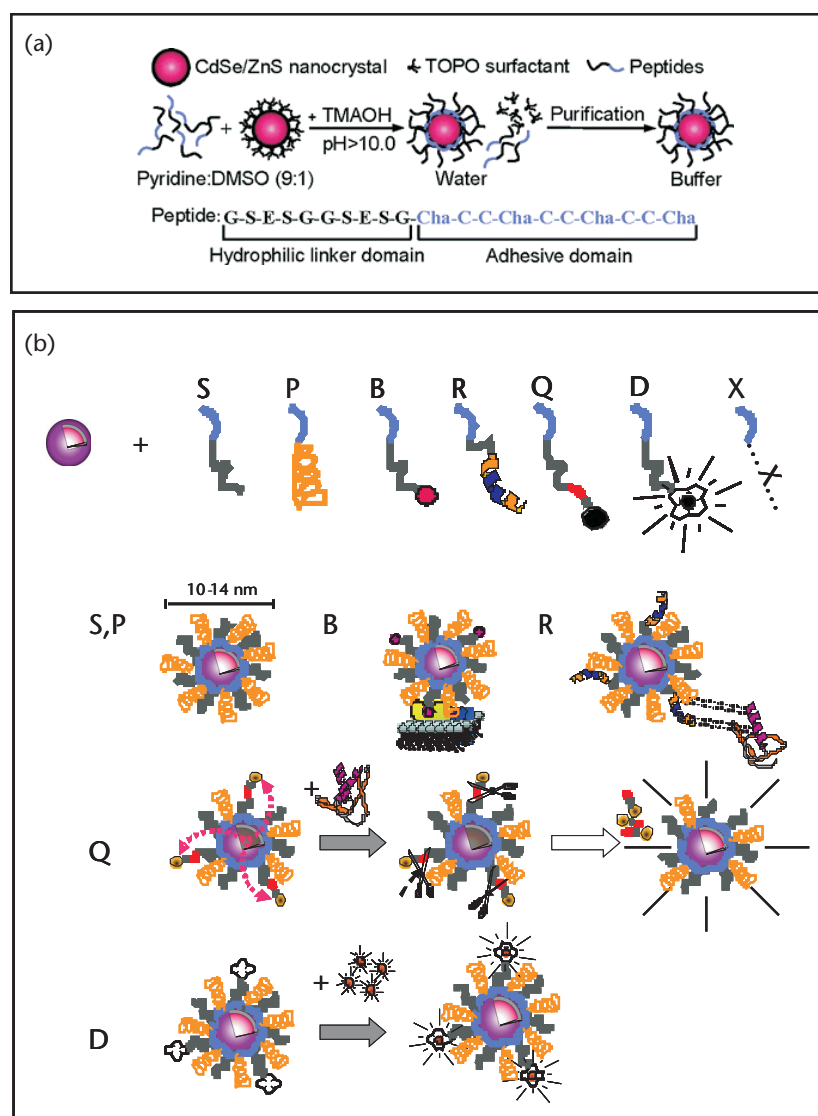


**Figure 3.2** The phytochelatin peptide-coating approach: (a) Schematic representation of the surface coating chemistry of CdSe/ZnS nanocrystals with phytochelatin-related -peptides. The peptide C-terminal adhesive domain binds to the ZnS shell of CdSe/ZnS nanocrystals after exchange with the trioctylphosphine oxide (TOPO) surfactant. A polar and negatively charged hydrophilic linker domain in the peptide sequence provides aqueous buffer solubility to the nanocrystals. TMAOH: Tetramethyl ammonium hydroxide; Cha: 3-cyclohexylalanine. Adapted from [19] with permission from American Chemical Society. (b) Schematic representation of the peptide toolbox. The light blue segment contains cysteines and hydrophobic amino acids ensuring binding to the nanocrystal (adhesive domain of Figure 3.2(a)) and is common to all peptides. S: solubilization sequence (hydrophilic linker domain of Figure 3.2(a)), P: PEG, B: biotin, R: recognition sequence, Q: quencher, D: DOTA (1,4,7,10-tetraazacyclododecane-1,4,7,10-tetraacetic acid) for radionuclide and nuclear spin label chelation, X: any unspecified peptide-encoded function. Qdots solubilization is obtained by a mixture of S and P. Qdots can be targeted with biotin (B), a peptide recognition sequences (R), or other chemical moieties. Qdots fluorescence can be turned on or off by attaching a quencher (Q) via a cleavable peptide link. In the presence of the appropriate enzyme, the quencher is separated from the qdot, restoring the photoluminescence and reporting on the enzyme activity (as described in Section 3.6). For simultaneous PET (or MRI) and fluorescence imaging, qdots can be rendered radioactive by chelation of radionuclides (or nuclear spin labels respectively) using (D) DOTA (as described in Section 3.5). Adapted from [5] with permission from American Association for the Advancement of Science. (See Color Plate 3.)

solid-phase peptide synthesis, which can also be technically challenging for cysteine-rich peptides.

**Table 3.1** Phytochelatin-Related  $\alpha$ -Peptides Used for Solubilization/Functionalization of Qdots

<i>Nomenclature</i>	<i>Peptide Sequences*</i>	<i>References</i>
1	KGSEGGSESG( <i>Cha</i> )CC( <i>Cha</i> )CC( <i>Cha</i> )CC( <i>Cha</i> )-Cmd	[19]
2	Biotin-GSEGGSESG( <i>Cha</i> )CC( <i>Cha</i> )CC( <i>Cha</i> )CC( <i>Cha</i> )-Cmd	Ibid
3	PEG-( <i>Cha</i> )CC( <i>Cha</i> )CC( <i>Cha</i> )CC( <i>Cha</i> )-Cmd	Ibid
4	GSEGGSESG( <i>Cha</i> )CC( <i>Cha</i> )CC( <i>Cha</i> )CC( <i>Cha</i> )-Cmd	Ibid
5	Ac-GSEGGSESG( <i>Cha</i> )CC( <i>Cha</i> )CC( <i>Cha</i> )CC( <i>Cha</i> )-Cmd	Ibid
6	Suc-GSSSGSSSG( <i>Cha</i> )CC( <i>Cha</i> )CC( <i>Cha</i> )CC( <i>Cha</i> )-Cmd	Ibid
7	FITC-GSEGGSESG( <i>Cha</i> )CC( <i>Cha</i> )CC( <i>Cha</i> )CC( <i>Cha</i> )-Cmd	[44]
8	GSEGGSESGFCCFCCFCF-HS <sup>b</sup>	Ibid

\*All sequences are written from N- to C-terminus. Cmd: carboxamide; Ac: N-terminal acetylation; Suc: N-terminal succinylation; *Cha*: 3-cyclohexylalanine (unnatural amino acid), PEG: hexaethyleneglycol. <sup>b</sup>HS: homoserine residue obtained after CNBr cleavage of methionine residue.

Contrary to the adhesive domain sequence that is fixed, the hydrophobic tail sequence is variable and can be altered at will to dial in desirable intracellular homing sequences and/or functional groups for bioconjugation (Figure 3.2(b)). The inherent flexibility of this approach provides endless functionalities (in the form of a “peptide toolbox”) that can be subsequently combined to create multimodal qdot imaging probes (later described in Section 3.5). But perhaps the main advantage for the experimentalist resides in the simplicity by which the peptide surface chemistry exchange is accomplished in a single reaction step (Figure 3.2(a)). The addition of tetramethylammonium hydroxide (TMAOH) base to a mixture of peptides:qdots in DMSO:pyridine (1:9) triggers the formation of cysteine thiolate anions, which initiates binding of the peptides onto the ZnS layer. The resulting peptide-coated nanoparticles precipitate out of the cosolvent and are collected by centrifugation. At this point, the qdots are readily soluble in aqueous buffers. Gel filtration and dialysis are then used to remove the excess of unbound peptides and to transfer the peptide-coated qdot in the appropriate buffer of choice. Table 3.1 lists some of the phytochelatin-related  $\alpha$ -peptide sequences used. Recently, Zheng et al. have successfully mimicked the use of a natural phytochelatin peptide by describing a facile one-pot aqueous synthesis of glutathione-coated CdTe qdots [45].

### 3.3 Colloidal and Photophysical Properties of Peptide-Coated Qdots

The peptide-coating approach overcomes some of the known limitations of other capping strategies that lead to particles that either lack long-term stability [2, 15], result in large particles [20, 21], have broader size distributions [1], or do not work well with all particle sizes [23]. Because of the organic nature of the peptide coat, which provides biocompatibility in aqueous buffer, conventional analytical techniques can be used to systematically monitor the ligand-exchange reaction’s efficiency. For example, we routinely use size exclusion liquid chromatography (SE-HPLC) and agarose gel electrophoresis as stringent criteria to test for batch quality and consistency. Such analysis is also instrumental in determining the size

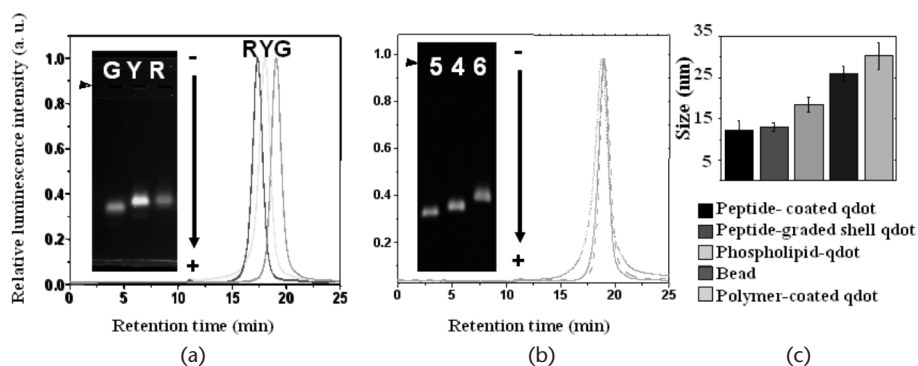


**Figure 3.3** Characterization of peptide-coated qdots: (a) Effect of qdot size as measured by SE-HPLC and gel electrophoresis. The nomenclature of the peptides refers to the numbering in Table 3.1. Green, yellow, and red qdots emitting at 530, 565, and 617 nm, respectively, and coated with peptide 5 were separated on a size exclusion column against a 0.1M PBS mobile phase. The diameter of the peptide-coated qdots was evaluated from the elution times as 129.4Å ( $\pm 15$  percent), 150.3Å ( $\pm 16$  percent), and 164.8Å ( $\pm 14$  percent), respectively. Inset: 0.5 percent agarose gel electrophoresis of the same three peptide-coated qdot samples in TBE buffer pH 8.3. (b) Effect of peptide charge. Qdots coated with peptide 5 (dash), peptide 4 (dot), or peptides 6 (solid) have similar retention times on a SE-HPLC column. Inset: the same peptide-coated qdots migrate at different positions on a 0.5 percent agarose gel, in good agreement with the theoretical charge of each peptide.  $\rightarrow$ : position of the loading wells.  $\leftarrow$ : direction of the applied electric field. (c) Effect of peptide charge on peptide-coated qdots. Qdots coated with peptide 5 (dash), peptide 4 (dot), or peptides 6 (solid) have similar retention times on a SE-HPLC column (same size) while having different charges as accessed by gel electrophoresis. Adapted from [19] with permission from American Chemical Society. (c) Hydrodynamic diameter of various qdot preparations deduced from FCS analysis. Adapted from [46] with permission from American Chemical Society. (See Color Plate 4.)

distribution range of the resulting peptide-coated qdots. Figure 3.3(a) illustrates how narrow the size distribution of a typical peptide-coated qdot batch can be. For example, the tight, smearless band in the agarose gel is indicative of the deposition of a uniform peptide layer of a constant thickness, independent of the original size of the nanoparticle's core-shell structure. Figure 3.3(b) shows also how subtle variations of the hydrophilic peptide sequence can result in changes of the overall particle charge that can be easily resolved by the electrophoretic process. SE-HPLC and FCS provide an estimate of the hydrodynamic radius of the coated nanoparticles. All together, the peptide-coating approach maintains the overall size of the qdots as relatively small (8 to 13 nm, Figure 3.3(c)) compared to  $\sim 18$  nm for phospholipid-coated qdots and up to 30 nm for commercial nanocrystals protected by a polymer coat as shown by FCS analysis [46]. This is definitely an advantage for cell biology applications in which interference with biological interactions and target inaccessibility due to steric hindrance need to be kept to a minimum.

Finally, peptide-coated qdots have long shelf lives and show minimum aggregation in physiological buffer over several months when kept at 4 degrees C. On the other hand, we observed that the quantum yield (QY) of the peptide-coated qdots in buffer is somewhat influenced by the composition and structure of the shell, ranging from 8–16 percent for CdSe/ZnS to 20–35 percent for CdSe/CdS/ZnS with graded

shells [5]. A graded shell composition also seems to induce a slight change of emission spectra (red shift) upon peptide coating. This is suggestive of cross-talks between the excitonic wavefunction and the peptide molecular orbitals [5]. One can envision that these sorts of interactions can be harnessed to improve the photo-physical properties of the peptide-coated qdots (e.g., as to enhance quantum yield or to reduce fluorescence intermittency by screening large libraries of peptides). Such strategies have been extremely powerful for the recognition, synthesis, and self-assembly of nanocrystals and other metallic materials in bio-engineered phase [36, 37, 47] or in bacteria [48].

## 3.4 Live Cell Dynamic Imaging

### 3.4.1 Single-Particle Tracking of Cell-Surface Membrane Receptors

As discussed previously, one of the advantages of the peptide-coating approach relies on those qdot surface properties that are easily controlled and tuned with various peptide combinations (Figure 3.2(b)). The peptide exchange chemistry can be modified to produce a large variety of functional groups that are exposed at the particle surface, allowing a number of covalent modification techniques for conjugation. In general, the presence of amines and/or thiols on the qdot surface enables the most common conjugation strategies [49, 50] and sidesteps the need to chemically prepare specialized linker molecules. For example, one can easily activate peptide-coated qdots with biotin. The qdots can also be directly coated with synthetic biotinylated peptides (peptide 2 in Table 3.1 and peptide B in Figure 3.2(b)) or via the conjugation of amine reactive biotinylation reagents (such as succinimidyl ester biotin) on a terminal lysine amino acid residue of peptide-coated qdots (peptide 1 in Table 3.1 and [51]). These biotin-terminated peptide-coated qdots show excellent reactivity with avidin, neutravidin, or streptavidin [19].

Importantly, this bioactivation approach maintains a small particle diameter, which is a valuable asset for targeting, detecting, and monitoring the trajectories of individual proteins in the plasma membrane of living cells. Their hydrodynamic radius ( $< 12$  nm, Figure 3.3(c)) is significantly smaller than the commonly used 40-nm gold nanoparticles or 500-nm latex beads that may interfere with protein dynamic [10, 52]. Qdots also outperform the rapid photobleaching of small (1- to 4-nm) fluorescent organic labels [10, 53]. For example, we have used biotin-terminated peptide-coated qdots to target avidin fusion to glycosylphosphatidylinositol CD14 cell surface receptor (CD14-Av) in cultured HeLa cells (Figure 3.4 and [19]). This approach not only demonstrated specific recognition of the CD14-Av proteins on the cell membrane, but also that qdot fluorescence can be used to track the movement of single receptors in live cells over extended period of time. Indeed, by working at subnanomolar concentration of biotin-peptide-coated-qdots to ensure that individual qdots could be distinguished optically, we were able to observe binding events and the subsequent membrane diffusion of individually labeled CD14-Av receptors, as illustrated in Figure 3.4.

The brightness and high saturation intensity of peptide-coated qdots [46, 54] allow the use of a standard CCD camera (CoolSnap *cf*, Princeton Instruments, Trenton, NJ) and rather short exposure times ( $\sim 100$  ms). Other experiments performed

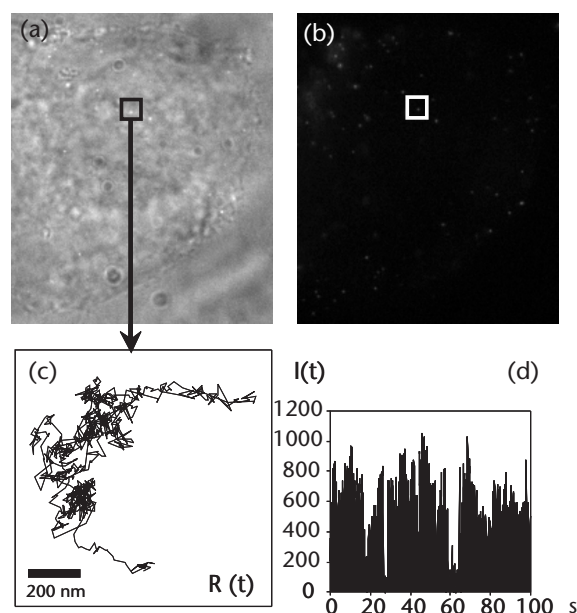


**Figure 3.4** Single-particle tracking in a live-cell: (a) DIC and (b) epifluorescence images of live HeLa cells expressing the CD14-Av receptors (see main text for details). Single qdots were observed to diffuse at characteristically different rates in different regions of the membrane or inside the cytosol (data not shown). (c) The 1,000 steps (100 ms/step) trajectory,  $R(t)$ , of the qdot localized in the region marked in panel (A, B), with (d) the corresponding qdot intensity,  $I(t)$ . The blinking pattern (succession of on and off emission) demonstrates that a single qdot was observed. Adapted from [5] with permission from American Association for the Advancement of Science.

with an electron multiplying camera (Cascade 512B, Princeton Instruments) and total internal reflection (TIR) microscopy allowed the use of much shorter exposure time (20 ms or less). It is worth mentioning that the trajectory of an individual receptor cannot necessarily be tracked continuously due to the intermittence in qdot's fluorescence emission (Figure 3.4(d)). Instead, we use this blinking behavior as a proof of singleness. The advantages of using qdots in these experiments become evident. Qdots' photostability can allow the observation of individual receptor trajectories for 10 to 20 min compared to  $\sim 5$ s with Cy3-labelled antibodies [10]. The brightness of the qdots also allows the spots to be detected with a high signal-to-noise ratio (SNR  $\sim 50$ ), while short integration time allows the capture of the full dynamic of the process. The high SNR allows better positioning accuracy ( $\sim 5$ – $10$  nm) of the tracked particle and its receptor. Similar experiments by Dahan et al. [10] tracking extra-synaptic receptors also revealed that these cell-surface proteins were far more mobile than previously considered by single-particle tracking using micrometer-sized beads [55], further confirming that the size of larger load does influence diffusion properties. Long trajectory observations give access to a wealth of information on the local spatio-temporal environment of each particle, which would be accessible only through statistical analysis of hundreds of trajectories using standard fluorescent dyes [56].

### 3.4.2 Peptide-Mediated Intracellular Delivery and Targeting of Qdots

The delivery of biological and/or inorganic cargos across the membrane lipid bilayer of living cells toward the cell interior has many potential applications that range from the development of novel therapeutic agents to the basic understanding of gene and protein functions. Mammalian cells have evolved strategies to selectively import and export vital compounds like hydrated ions and small polar molecules. But the plasma membrane still represents a formidable barrier to the passage of larger biomolecules. Colloidal qdots consisting of an inorganic core surrounded by a layer of organic ligands resemble proteins both in term of size (in the nanometer range) and charge (negative) and thus do not freely diffuse across the lipid bilayer of live cells. For these reasons, the use of qdots has principally focused on targeting cell surface membrane markers that are easily accessible from the surrounding culture medium. The use of electroporation or transfection reagents [57] that capitalize on a receptor-mediated endocytotic translocation routes results in qdots being sequestered and accumulating in lysosomal and endosomal vesicles that appear scattered in the cytoplasm [58, 59]. On the other hand, the direct microinjection of peptide-conjugated or peptide-coated qdots in living cells [51, 57] has allowed the targeting of qdots to subcellular compartments such as mitochondria [57] or the nucleus [60]. All of these physical approaches have, however, limited in vivo applications since they are serial, time consuming, or technically challenging, and they do not allow high-throughput screening. Thus, there is still a need to systematically explore various strategies for delivering qdots into live cells, especially those that can facilitate cell entry without the requirement for endocytosis.

To date, the use of short arginine-rich peptide sequences constitutes one of the most promising classes of ligands for the intracellular delivery of a variety of macromolecules into live cells [61] including qdots [58, 60, 62–69]. These sequences, referred to as *cell permeable peptides/peptide transduction domains* (CPP/PTD), include short segments first isolated from the human immunodeficiency virus 1 (HIV-1) transcriptional activator Tat protein, the *drosophila* homeotic transcription protein antennapedia (Antp), and the herpes simplex virus structural protein VP22 [70]. Other sequences have been identified, including homopolymers of arginine [71]. Most, if not all, PTDs carry a net positive charge (highly rich in basic residues), are less than 20–30 amino acids long, and have the ability to rapidly translocate large molecules into cells. PTDs that have been used for intracellular delivery of qdots are shown in Table 3.2.

While the mechanism responsible for uptake of PTDs and their cargos remains unclear, if not controversial, PTDs can be used to accelerate the intracellular delivery of qdots into a variety of cell types by coupling PTDs to qdots via a streptavidin-biotin link [21, 58, 60], covalently [72], by electrostatic adsorption of PTDs containing free cystein residues [57] or not [73]. Once mono-disperse qdots are given access to the cytosol, they can be delivered to specific cellular compartments or organelles by means of different homing peptide sequences (residue R in Figure 3.2(b)). This has been elegantly demonstrated for targeting peptide-qdot conjugates to the mitochondria [57] and the nucleus [57, 60].

**Table 3.2** Protein Transduction Domains Used for Intracellular Delivery and Targeting of Qdots

<i>Localization</i>	<i>Peptide Sequences*</i>	<i>References</i>
Cytoplasmic	RRRRRRRRR	[58, 59]
	(His) <sub>8</sub> -WGLA(A <sub>ib</sub> )SG(R) <sub>8</sub>	[67]
	RKKRRYRRR	[21]
	KETWWETWWTEWSQPKKKRKV	[73]
Nuclear	PPKKKRKVPKKKRKV	[60]
	CSSDDEATADSQHSTPPKKKRKV	[57]
	RRRRRRRRRRRKC	[72]
	APSGAQRLYGFGL	[74]
Mitochondrial	MSVLTPLLLRGLTGSARRLPVPRAKIHC	[57]
	MSVLTPLLLRGLTGSARRLPVPRAKIHWLC	[72]

\*All sequences are written from N- to C-terminus. (His)<sub>8</sub>: polyhistidine, A<sub>ib</sub>: alpha-amino isobutyric acid.

### 3.5 Live Animal Imaging

The visual analysis of molecules and cellular processes in living subjects (i.e., molecular imaging) has the potential to markedly enhance earlier diagnosis of disease. Radionuclide tracers and 3-D imaging systems such as positron emission tomography (PET) and single photon emission computed tomography (SPECT) are now helping to characterize the molecular status of tumors in patients [75]. While effective, the use of radiopharmaceuticals is limited by their complex fabrication, the short half-life of the isotopes as well as other issues related to patient/provider safety, and radioactive waste disposal. The use of radioactivity-based methods is further impaired by the inability to multiplex simultaneous signals and by the lack of detection sensitivity toward small tumor burdens. (For a review, see [76].) The other alternative in deep tissue imaging relies on multiphoton fluorescence microscopy, which can capture high-resolution, 3-D images of living tissues tagged with highly specific fluorophores [77]. However, tissue absorption and scattering, in addition to limiting the light coming out of the subject, also limits the amount of incident excitation light that reaches the fluorophore. As a result, only a very limited amount of excitation light becomes available at deeper regions of the animal tissue.

Finally, conventional dye molecules suffer major limitations that include poor photostability and phototoxicity. In this section, we review how qdots provide highly sensitive alternatives to both radioactivity- and fluorophore-based methods. First, we demonstrate how the peptide-coating approach allows the tens to hundreds of nm<sup>2</sup> of qdots' surface area to be functionalized with a combinatorial assortment of different peptide sequences to make radiolabeled qdots for dual-modality imaging (both fluorescence and PET in a single probe). Then we show how small peptides are paving the way for the first successful targeted deliveries of qdot conjugates in live animals. This growing trend is confirming their unmatched potential as novel intravascular probes for deep-tissue imaging in various optical modalities, including two-photon confocal microscopy [6], PET [5, 78, 79], and SPECT/CT [80].

### 3.5.1 Near-Infrared Deep-Tissue Dual-Modality Imaging

The complex nature of mammalian tissues, through which photons are absorbed and scattered, generally limits the depth at which light-emitting probes can be imaged *in vivo* [81, 82]. One partial remedy is to rely on near infrared (NIR) wavelengths for excitation and/or emission. At 700 nm to 900 nm, the absorbance of all biomolecules reaches a minimum while maximizing photon penetration efficiency into and out of tissues. This provides a clear window with minimal autofluorescence for *in vivo* optical imaging [83]. In the past five years, the contribution of NIR qdots to this biologically relevant “therapeutic window” [84, 85], where no good fluorescent dyes exist, has been quite remarkable. For example, Kim et al. have demonstrated in pigs and mice the superiority of NIR qdots in sentinel lymph node (SLN) mapping, a major procedure in breast cancer surgery. Qdots allowed real-time image guidance throughout the procedure, virtually free of any background, 1 cm deep into the tissues [86]. These and others studies have established the great potential of qdot optical imaging as a surrogate to radioactive techniques [6, 21].

On the other hand, only radioactive tracers have the unique ability to provide both quantitative *in vivo* biodistribution and deeper imaging data. Based on these considerations, our laboratory created the first dual-mode qdot probe combining optical and radioactive imaging capabilities [5]. For simultaneous PET and fluorescence imaging, qdots were radiolabeled by chelation of a radionucleotide ( $\text{Cu}64$ ) to a DOTA (1,4,7,10-tetraazacyclododecane-1,4,7,10-tetraacetic acid) functionalized peptide (peptide D in Figure 3.2(b)). Polyethylene glycol moieties of various lengths (PEG, peptide 3 in Table 3.1 and peptide P in Figure 3.2(b)) were also added in a single-step reaction in an attempt to reduce nonspecific binding and increase blood circulation time [87]. These radiolabeled qdots were injected ( $\sim 80 \mu\text{Ci}$  per animal) via tail-vein into anesthetized nude mice and then dynamically imaged in a small animal mPET scanner (Concorde Microsystems Inc., Knoxville, TN). Biodistribution and mPET analysis showed rapid and marked hepatic and splenic uptake of the qdots without evidence of body clearance (Figure 3.5(a)). This known tendency is caused by specialized particle-scavenging Kupffer cells residing en masse in the reticulo-endothelial system (RES) of the liver and spleen [87]. We also observed that PEGylation beneficially increased the blood circulation half-life and somewhat slowed down liver and spleen uptake of qdots [78]. Here, one clear advantage of the

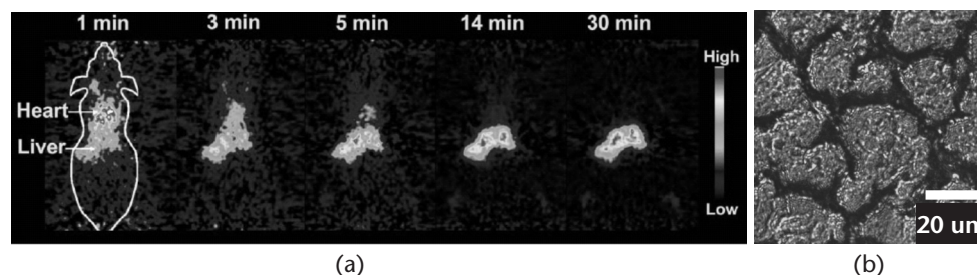


**Figure 3.5** Dual-mode imaging in live animals: (a) sPET imaging of nude mice injected with radiolabeled qdots through a DOTA-functionalized peptide (see Section 3.5 for details). (b) Overlay of DIC and fluorescence images of hepatocytes from a mouse showing the accumulation of qdots within liver cells. Scale bar indicates  $20 \mu\text{m}$ . Adapted from [5] with permission from the American Association for the Advancement of Science.

peptide-coating approach is that it gives us considerable latitude to modulate parameters such as peptide density and thus the overall number of functional groups (i.e., PEG moieties) or the overall charge (as shown in Figure 3.3(b)). Separate studies where free copper chloride ( $\sim 78 \mu\text{Ci}$ ) is injected via tail-vein show that the maximum signal in the liver is only 7.8 percent of that observed when injecting mice with Cu64 radiolabeled peptide-qdots ( $\sim 80 \mu\text{Ci}$ ). This demonstrates that even if all of the copper/peptide dissociates from the qdots, it can only lead to a small component of the overall liver signal. Moreover, biopsies of the liver observed by fluorescence light microscopy confirm this accumulation of qdots within the liver (Figure 3.5(b)).

It is important to realize that fluorescence alone cannot be measured in a fully quantitative way due to the scattering and absorption properties of living tissues as mentioned previously. There are multiple benefits to having dual-mode radioactive and optical peptide-coated qdots. First, this combination allows fluorescence imaging of qdots for tracking together with quantitative biodistribution studies of the radiotracer to access accurately their pharmacokinetics and targeting efficacy in living animals. Second, the dual-modality approach requires a much smaller amount of qdots (in our studies:  $\sim 25 \text{ pmol}$  or  $0.8\text{--}1.25 \text{ nmol/kg}$  depending on the weight of the animal [78]) to yield enough contrast for PET imaging than optical imaging alone (about 10 to 100 times more qdots needed). This can significantly lower the potential cyto-toxicity risk posed by  $\text{Cd}^{2+}$  and other heavy metals leakage from the qdot inner core structure [88, 89]. Nuclear spin labels for MRI imaging could also be incorporated into qdots peptide coating using the same type of chelating group. A further step could involve TEM imaging of their precise localization within cells and tissues [10, 90]. It should therefore be possible to image targeted qdots at all scales, from the level of whole body down to the nanometer resolution using a single probe with exquisite spatio-temporal sensitivity.

### 3.5.2 In Vivo Targeting of Tumor Vasculature

To date, the successful targeted delivery of peptide qdots in living mice has been limited to tissue-specific vascular markers. Akerman et al. have used lung- and tumor-specific homing peptides (Table 3.3) to direct qdots to their appropriate targets. After intravenous injection in the mice, targeting was demonstrated by ex vivo fluorescence microscopy of histological sections [18]. However, no in vivo imaging was achieved. More recently, arginine-glycine-aspartic acid (RGD) peptide-conjugated qdots have been used to specifically target integrin  $\alpha_v\beta_3$  in vitro [91, 92] and in living mice [63, 79]. The RGD peptide motif (Table 3.3) found in vitronectin, fibronectin, and thrombospondin [93] binds selectively to integrin  $\alpha_v\beta_3$ . Taking advantage of the fact that integrin  $\alpha_v\beta_3$  is significantly upregulated in tumor but not in normal tissues [94, 95], Cai et al. reported the first in vivo targeting and imaging of tumor vasculature in a murine xenograph model in live animals using RGD-qdot conjugates [63, 79]. Subcutaneous tumor imaging was observed six hours post-injection (Figure 3.6(a)) and was further demonstrated by harvesting the tumor followed by ex vivo imaging using a sensitive CCD camera (IVIS200, Xenogen Corp., Alameda, CA). Qdot fluorescence signal was clearly detected in the tumor of the mouse injected with the RGD qdots, while no signal was seen in the

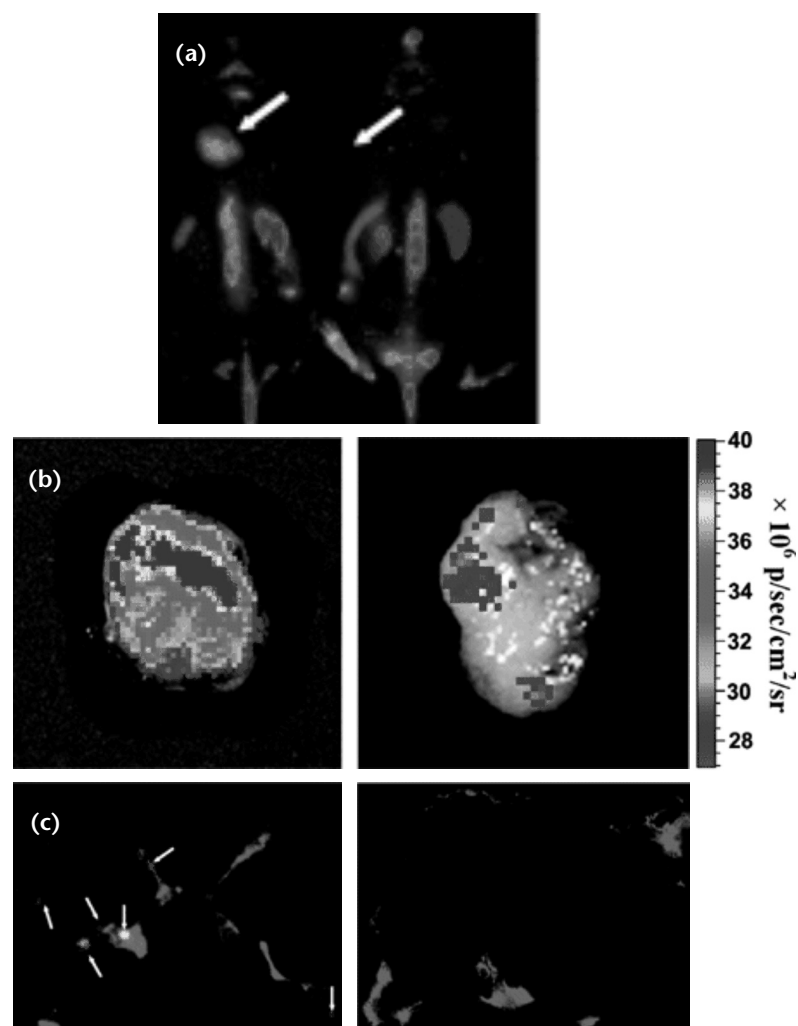


**Figure 3.6** Targeting of tumor vasculature with RGD peptide-conjugated qdots: (a) In vivo NIR fluorescence imaging of U87MG tumor-bearing mice (left shoulder, pointed at with white arrows) injected with 200 pmol of RGD-qdots (left mouse) and control qdots (right mouse) six hours after injection. (b) Ex vivo fluorescence images of the same tumors, surgically removed from RGD qdots (left) and control qdots (right) injected mice. (c) Fluorescent microscope images of frozen tumor slices stained for CD31 (green) to allow visualizing of the tumor vasculature. Qdot signal is shown in red and pointed at with white arrows. Adapted from [63] with permission from the American Chemical Society. (See Color Plate 5.)

tumor of the control mouse injected with qdots alone (Figure 3.6(b)). Interestingly, further fluorescence microscopy analysis of frozen sections indicated that the RGD qdots did not extravasate but stayed confined to the tumor vasculature (Figure 3.6(c)) as previously reported [18]. Overall, the advantages for using peptide qdots for tumor targeting in vivo are multiple. Compared to their peptide-dye conjugate counterparts (RGD-Cy5.5, [96]) RGD qdots showed more photostability and much stronger signal-to-background ratio. In conjunction with other specific integrin binding peptides (RGDS, LDV, DGEA, KGD, PECAM, and FYFDLR), qdots offer

the unique possibility of multiplexing [91]. Peptides might also potentially be better targeting ligands than mono-clonal antibodies conjugated to qdots. Gao et al. estimated that the number of antibodies per qdots is limited to 5–6 [21], while the number of peptides can easily be optimized to provide stronger binding avidity [19]. Peptides might also be rendered multimeric to improve targeting efficiency because of the polyvalency effect [97–99]. The next step remains to improve tumor-targeting efficacy, which requires extravasation of the peptide-qdot probe as opposed to targeting the tumor vasculature where no extravasation is needed. Reducing the size of the qdot probes will lower uptake by the reticulo-endothelial system (RES), which holds the key to achieving better tissue penetration and tumor targeting.

**Table 3.3** Sequences of Homing Peptides Used for In Vivo Targeting

<i>Vasculatures</i>	<i>Peptide Sequences*</i>	<i>References</i>
Lung	CGFECVRQCPERC	[18]
Tumor, blood	KDEPQRRSARLSAKPAPPKPEPKKKAPAKK	Ibid
Tumor, lymphatic	CGNKRTRGC	Ibid
Integrin $\alpha_v\beta_3$ tumor	RGD	[63, 79]

\*All sequences are written from N- to C-terminus.

## 3.6 Beyond Diagnostic Imaging: Sensing and Therapeutics Applications

Optical sensing (i.e., detection of electromagnetic radiation) is the most widely used format for detecting biological binding events and enzymatic reactions or performing quantitative immunoassays in biological systems. The goals of using qdots are ultimately to enable single-molecule detection in vivo, parallel integration of multiple signals (i.e., multiplexing), signal amplification, and resistance to photobleaching in a high-throughput format. In the following section, we review some of the most significant progress in the application of peptide qdots in biological detection.

### 3.6.1 Cleavable Peptides for Proteases Activity

Proteases are enzymes that regulate many essential biological processes by catalyzing the cleavage of specific peptide bonds in other proteins. They are also well known to be aberrantly regulated and activated in various diseases including cancer, stroke, and infection [100]. Hence, proteases constitute a prominent class of pharmaceutical targets for assay and drug development. For example, because protease activity is key to tumor progression and evasion (metastasis), monitoring their expression and bioactivity in vivo provide information about the metastatic potential of a tumor. Many of the sensors designed to monitor proteolytic activity exploit the low background of FRET quenched fluorophores and the high fluorescent signal resulting from unquenching after proteolysis [101]. In such FRET geometry, two fluorophores are usually held in close proximity by a short peptide linker that becomes the target of a specific protease. The main limitations of these fluorophore-based probes reside in their lack of general tunability in wavelength, which is imposed by the donor-acceptor pair. In addition, the optical properties of

conventional organic fluorophores or genetically encoded fluorescent proteins are susceptible to their local environment (pH sensitivity and so on) and prone to photobleaching. In order to overcome some of these shortcomings, qdot-peptide conjugates have emerged as promising new FRET-based protease sensors. The use of qdots as energy donors capitalizes on their well-known spectroscopic benefits. Specifically relevant here is their broadband absorption and fluorescence emission spectra that can be tuned to best overlap with the acceptor absorption. With this in mind, Chang et al. designed the first qdot-peptide-gold conjugates to target collagenase. In this bioassay, collagenase cleaves between alanine and glycine of a GGLGPAGGCG target peptide to release the functionalized gold nanoparticles that quenches the qdot fluorescence [102]. This approach was however limited by steric hindrance from the gold nanoparticles, which impaired the accessibility of the collagenase to the peptide.

As an improvement of this approach, Medintz et al. have developed qdot-peptide-dye conjugates for the enzyme recognition of four different target enzymes (Table 3.4); caspase 1, thrombin, collagenase, and chymotrypsin [103]. Replacing gold with a much smaller dye molecule (Cy3 or QXL-520) possibly increased the substrate accessibility to the protease since the authors succeeded in measuring kinetic values similar to those obtained with dye-only peptides in solution. Steric constraints were also minimized by titrating the peptide-qdot ratio to be less than 5. Moreover, the low peptide number ensures that the proteolytic assays were carried out under rate-limiting substrate conditions, which means that all peptides on the qdots are likely to participate in the protease activity measurement. The net result is an increase in the sensitivity of the QD-peptide-dye probes. Finally, these QD-peptide sensors can also measure protease activity *in vivo*. Shi et al. used qdots directly coated with a small RGDC tetrapeptide labeled with rhodamine to quantitatively study the aberrant collagenase activity of HTB 126 cancer cell lines [104]. The kinetic rate constants of FRET signal changes of the qdot-based protease sensors were significantly higher within the cancer cells as compared to the normal HTB 125 cells. Interestingly, the qdot FRET-based probes could discriminate between normal and cancerous cells within 10 min. By extension, changing the peptide sequence would enable high throughput screening of the activity of specific proteolytic enzymes in real-time in an array/multiplex format. This could provide a unique protease signature for each cancer patient to personalize ongoing therapeutic strategies.

**Table 3.4** Sequences of Cleavable Peptides Used for Measuring Protease Activity

<i>Target Enzymes</i>	<i>Peptide Sequences*</i>	<i>References</i>
Collagenase	GGLGPAGGCG	[102]
	RGDC	[104]
	(His) <sub>6</sub> -AL(A <sub>ib</sub> )AAGGPAC	[103]
Caspase-1	(His) <sub>6</sub> -GL(A <sub>ib</sub> )AAGGWEHDSGC	Ibid
Thrombin	(His) <sub>6</sub> -GLA(A <sub>ib</sub> )SGFPRGRC	Ibid
Chymotrypsin	(His) <sub>6</sub> -GL(A <sub>ib</sub> )AAGGWGC	Ibid

\*All sequences are written from N- to C-terminus. (His)<sub>6</sub>: polyhistidine, A<sub>ib</sub>: alpha-amino isobutyric acid.

### 3.6.2 Photodynamic Therapy

Photodynamic therapy (PDT) refers to a kind of cancer treatment based on three synergistic components: a photosensitizer (PS), light, and oxygen molecules present in tissues [105, 106]. Photosensitizers are nontoxic chromophores that generate reactive oxygen species (ROS) such as free radicals (hydroxyl radical:  $\bullet\text{OH}$  and superoxide:  $\bullet\text{O}_2^-$ ) and single oxygen ( $^1\text{O}_2$ ) upon light irradiation. These compounds act locally to cause irreversible oxidative damages to enzymes, proteins, nucleic acids, mitochondria, and membranes with the result of inducing apoptosis, necrosis, and cell death. In the clinic, the effectiveness of a PDT treatment relies on the retention and accumulation of the PS into tumor tissues followed by its selective destruction by ROS generated through laser irradiation of specific wavelength and directed to the sensitized local area. Compared with conventional surgery, this approach is minimally invasive. However, current FDA-approved PSs (such as Photofrin) are far from being ideal. They are poorly soluble, unstable, have low targeting selectivity, and show some spontaneous skin phototoxicity triggered by regular daylight (which goes with the fact that their excitation wavelengths are not optimal for deep tissue penetration). Given these major drawbacks, qdots have garnered much attention as potentially novel PSs or, at least, as cofactors of conventional PSs [107, 108]. Qdots main benefits relate to their resistance to photobleaching, emission, and absorption tunability in the NIR for deep tissue excitation, large absorption coefficients, continuous absorption bands that can be used to extend the range of excitation of conventional PSs through Förster (fluorescence) resonance energy transfer (FRET), and the availability of active-targeting approaches to introduce a degree of selectivity in PDT treatments. Qdots as PS carriers could boost singlet oxygen yield (through FRET) for better PDT efficacy over PSs alone. They also have the potential to act as imaging and therapeutic agents simultaneously.

Early attempts to harness the full capabilities of qdots in PDT have been limited due to the poor solubility and/or instability of the qdot-PS conjugates in the aqueous environment [109–111]. We recently developed novel qdot-PS bioconjugates based on our unique phytochelatin peptide-coating technology that preserved both the photophysical properties of the qdots and of the PSs [112]. Figure 3.7 describes the conjugation schemes used to covalently attach two PSs, rose bengal and chlorin e6, to phytochelatin peptides (peptide 1 in Table 3.1). The versatility of our mix-and-match peptide approach allowed us to carefully control the number of PSs conjugated to the qdots by simply changing the stoichiometry of PS-conjugated peptides to peptides of other functionalities (PEG, biotin, and so on; see Figure 3.2(b)) during the mass exchange process. Typically, 1 to 30 PSs could be grafted per qdots. It is worth mentioning that the number of PSs directly correlated with the size (i.e., surface area) of the qdots; the bigger the qdots, the more PSs could be added [112]. FRET was evident between the qdots (acting as donors) and PSs (acting as acceptors). Figure 3.7(c) shows the dramatic increase of fluorescence of both rose bengal (attached to green qdots) and chlorin e6 (attached to red qdots) as a result of FRET (red curve) in comparison with the fluorescence of PSs alone at the same concentration (black curves). An important conclusion is that the peptide coating layer is thin enough to allow easy energy transfer between qdots and the PSs. Finally, we found that the qdot-PS conjugates produced singlet oxygen either by exciting the PS

62 Peptide-Functionalized Quantum Dots for Live Diagnostic Imaging and Therapeutic Applications

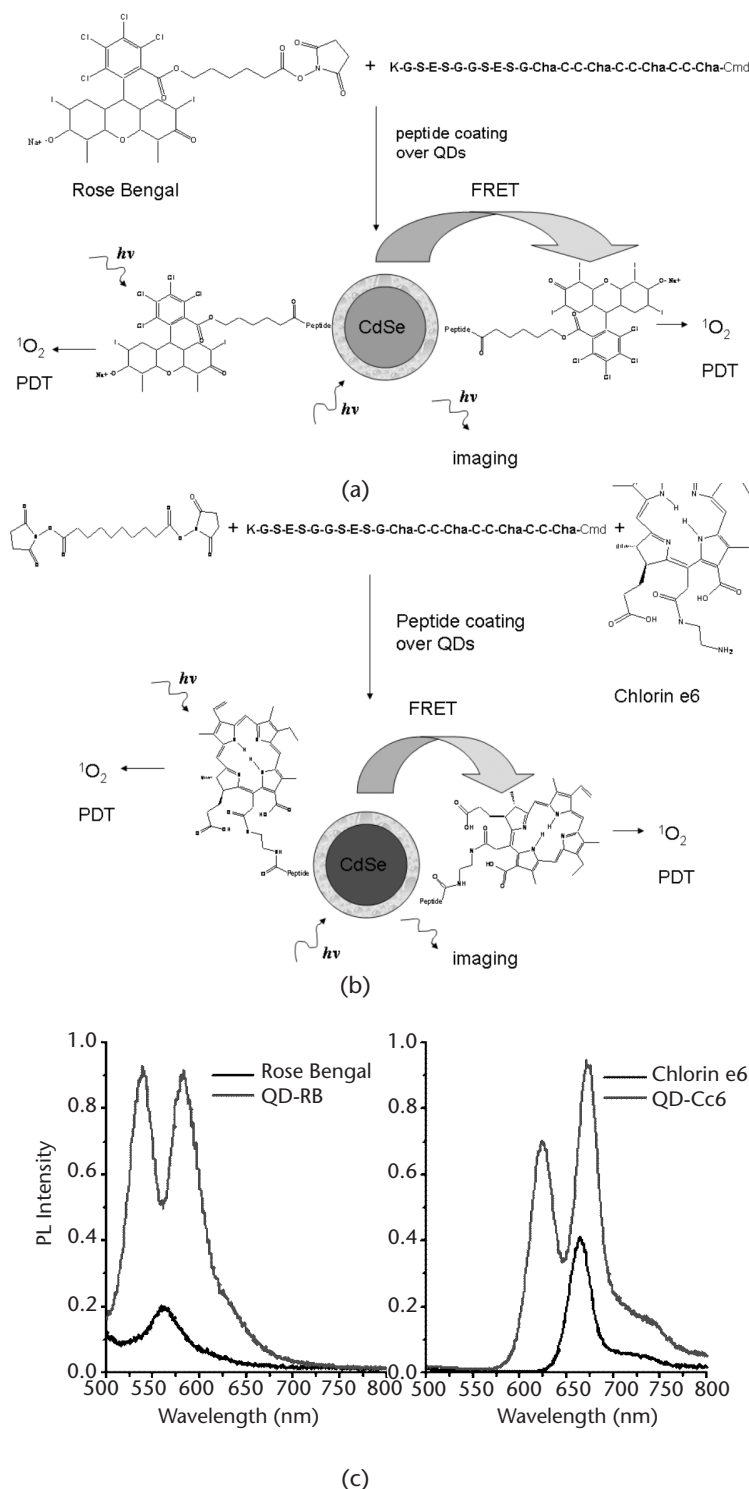


**Figure 3.7** Production of singlet oxygen with peptide-coated qdot-photosensitizer probes: (a) Scheme of conjugations of rose bengal and (b) chlorin to phytochelatin peptides. (c) Photoluminescence spectra of the conjugates. (left) rose bengal peptide-coated qdots (gray curve) and rose bengal alone (black curve). (right) Chlorin e6-conjugated QDs (gray curve) and chlorin e6 alone (black curve). The same concentration of each photosensitizer was excited at 450 nm. Adapted from [112] with permission from the American Chemical Society.

directly or indirectly through the FRET process. We are currently testing these qdot-PS conjugates for their ability to kill cells in culture. The next step would be to customize multifunctional qdot-PS probes able to specifically target cancer cells, absorb large quantities of light, and destroy tumors through singlet oxygen generation deep into tissue using NIR qdots and conjugation to NIR-absorbing photosensitizers.

### 3.7 Conclusion and Perspectives

Several key features make the peptide-coating approach advantageous for biological applications of qdots. First and foremost is its simplicity, since a single, simple reaction step can achieve both solubility in aqueous environment and bioactivation of the nanoparticles. Second, this approach is highly versatile and allows the testing of various peptide sequences simultaneously to encode multifunctional and multimodal capabilities in a single probe. Finally, the peptide-based approach maintains the overall size of the qdot probe as relatively small. For example, it has recently been demonstrated that a small ( $< 5$  nm) hydrodynamic radius is crucial for renal clearance of qdots intravenously injected into mice [113]. Without a way to excrete or biodegrade qdots into inert components, toxicity becomes an issue and imaging is impaired. Fortunately, the “peptide toolbox” gives us considerable latitude to modulate parameters such as peptide density, overall charge, hydrophilicity/hydrophobicity, and incorporation of moieties like high molecular PEG. In particular, PEG helps to increase biocompatibility, to neutralize nonspecific adsorption of serum proteins, and to increase circulation time in vivo. Therefore, peptide engineering might provide a rational path to the optimization of the pharmacokinetic parameters of IV-administrated functionalized qdots, while maintaining the final size of the functionalized probes as small as possible. Future research utilizing smaller, NIR-emitting qdots such as InAs-based qdots [114] may further promote extravasations of the qdots from the blood vasculature to target solid tumors. Active targeting strategies using peptides could also be combined with cytotoxic agents in the form of photodynamic therapy treatments.

At the cellular level, peptides offer wide potentials for novel applications. New affinity pairs will certainly emerge from in vitro directed molecular evolution to enable multiplexing studies [115]. New peptide sequences will facilitate crossing the cell membrane to go beyond the study of cell surface membrane markers to intracellular processes such as trafficking and signal transduction. Interestingly, recent studies are making use of extracellular proteases to modulate the cellular uptake of peptide-conjugated qdots [116]. Modulating the uptake of nanoparticles into cells with tumor-specific proteases may lead to their selective accumulation in tumor cells for further targeted destruction. Finally, new peptide qdot-based systems will be capable of sensing at the single-molecule level. Capitalizing on the advantages of both peptides and qdots may bring us closer to the ultimate goal of probing biological systems at all length scales: from the whole-body down to the cellular and molecular level with a single probe.

## Acknowledgments

We would like to thank our valuable colleagues in the field and ask for their forgiveness if some of their studies could not be cited within the space limits of this review. The development of the peptide-coated qdots was made possible thanks to the contribution of past and present members of our laboratory. Finally, we would like to express our appreciation to Tal Paley for her editorial assistance. Fluorescent microscopy images in Figure 3.5 were obtained at the California NanoSystems Institute Advanced Light Microscopy/Spectroscopy Shared Facility at UCLA. This work was supported by funds from the National Institute of Health, Grant No. 2 R01 EB000312-06A2.

## References

- [1] Bruchez, M.P., et al., "Semiconductor nanocrystals as fluorescent biological labels," *Science*, 1998. 281: 2013–2015.
- [2] Chan, W.C.W. and S.M. Nie, "Quantum dot bioconjugates for ultrasensitive nonisotopic detection," *Science*, 1998. 281(5385): 2016–2018.
- [3] Alivisatos, P., "The use of nanocrystals in biological detection," *Nat. Biotechnol.*, 2004. 22(1): 47–52.
- [4] Medintz, I.L., et al., "Quantum dot bioconjugates for imaging, labelling and sensing," *Nat. Mater.*, 2005. 4(6): 435–46.
- [5] Michalet, X., et al., "Quantum dots for live cells, in vivo imaging, and diagnostics," *Science*, 2005. 307(5709): 538–44.
- [6] Larson, D., et al., "Water-soluble quantum dots for multiphoton fluorescence imaging in vivo," *Science*, 2003. 300: 1434–1436.
- [7] Bharali, D.J., et al., "Folate-Receptor-Mediated Delivery of InP Quantum Dots for Bioimaging Using Confocal and Two-Photon Microscopy," *Journal of the American Chemical Society*, 2005. 127(32): 11364–11371.
- [8] Ferrara, D.E., et al., "Quantitative 3D fluorescence technique for the analysis of en face preparations of arterial walls using quantum dot nanocrystals and two-photon excitation laser scanning microscopy," *American Journal of Physiology*, 2006. 290(1, Pt. 2): R114–R123.
- [9] Serrano, E.E. and V.B. Knight, "Multiphoton imaging of quantum dot bioconjugates in cultured cells following Nd: YLF laser excitation," *Proceedings of SPIE-The International Society for Optical Engineering*, 2005. 5705(Nanobiophotonics and Biomedical Applications II): 225–234.
- [10] Dahan, M., et al., "Diffusion dynamics of glycine receptors revealed by single-quantum dot tracking," *Science*, 2003. 302(5644): 442–445.
- [11] Lidke, D.S., et al., "Reaching out for signals: filopodia sense EGF and respond by directed retrograde transport of activated receptors," *J. Cell Biol.*, 2005. 170(4): 619–626.
- [12] Warshaw, D.M., et al., "Differential labeling of myosin V heads with quantum dots allows direct visualization of hand-over-hand processivity," *Biophys. J.*, 2005. 88(5): L30–L32.
- [13] Bentolila, L.A., X. Michalet, and S. Weiss, "Quantum optics: colloidal fluorescent semiconductor nanocrystals (quantum dots) in single-molecule detection and imaging," *Single-Molecules and Nanotechnology*, R. Rigler and H. Vogel, Editors. 2008, Springer-Verlag: Heidelberg, pp. 53–81.
- [14] Yin, Y. and A.P. Alivisatos, "Colloidal nanocrystal synthesis and the organic-inorganic interface," *Nature*, 2005. 437(7059): 664–670.

- [15] Pathak, S., et al., "Hydroxylated quantum dots as luminescent probes for in situ hybridization," *J. Am. Chem. Soc.*, 2001. 123(17): 4103–4104.
- [16] Kim, S. and M.G. Bawendi, "Oligomeric Ligands for luminescent and stable nanocrystal quantum dots," *J. Am. Chem. Soc.*, 2003. 125(48): 14652–14653.
- [17] Guo, W., et al., "Conjugation chemistry and bioapplications of semiconductor box nanocrystals prepared via dendrimer bridging," *Chem. Mater.*, 2003. 15(16): 312–3133.
- [18] Akerman, M.E., et al., "Nanocrystal targeting in vivo," *Proc. Natl. Acad. Sci. USA*, 2002. 99(20): 12617–12621.
- [19] Pinaud, F., et al., "Bioactivation and Cell Targeting of Semiconductor CdSe/ZnS Nanocrystals with Phytochelatin-Related Peptides," *J. Am. Chem. Soc.*, 2004. 126: 6115–6123.
- [20] Wu, X.Y., et al., "Immunofluorescent labeling of cancer marker Her2 and other cellular targets with semiconductor quantum dots," *Nature Biotechnol.*, 2003. 21(1): 41–46.
- [21] Gao, X., et al., "In vivo cancer targeting and imaging with semiconductor quantum dots," *Nature Biotechnol.*, 2004. 22: 969.
- [22] Gerion, D., et al., "Synthesis and properties of biocompatible water-soluble silica-coated CdSe/ZnS semiconductor quantum dots," *J. Phys. Chem. B*, 2001. 105(37): 8861–8871.
- [23] Dubertret, B., et al., "In vivo imaging of quantum dots encapsulated in phospholipid micelles," *Science*, 2002. 298(5599): 1759–1762.
- [24] Gao, X., W.C.W. Chan, and S. Nie, "Quantum-dot nanocrystals for ultrasensitive biological labeling and multicolor optical encoding," *J. Biomed. Opt.*, 2002. 7(4): 532–537.
- [25] Pellegrino, T., et al., "Hydrophobic nanocrystals coated with an amphiphilic polymer shell: A general route to water soluble nanocrystals," *Nano Lett.*, 2004. 4(4): 703–707.
- [26] Osaki, F., et al., "A Quantum Dot Conjugated Sugar Ball and Its Cellular Uptake. On the Size Effects of Endocytosis in the Subviral Region," *J. Am. Chem. Soc.*, 2004. 126: 6520–6521.
- [27] Mattoussi, H., et al., "Self-assembly of CdSe-ZnS quantum dot bioconjugates using an engineered recombinant protein," *J. Am. Chem. Soc.*, 2000. 122(49): 12142–12150.
- [28] Sukhanova, A., et al., "Biocompatible fluorescent nanocrystals for immunolabeling of membrane proteins and cells," *Anal. Biochem.*, 2004. 324(1): 60–67.
- [29] Mitchell, G.P., C.A. Mirkin, and R.L. Letsinger, "Programmed assembly of DNA functionalized quantum dots," *J. Am. Chem. Soc.*, 1999. 121(35): 8122–8123.
- [30] Goldman, E.R., et al., "Conjugation of luminescent quantum dots with antibodies using an engineered adaptor protein to provide new reagents for fluoroimmunoassays," *Anal. Chem.*, 2002. 74(4): 841–847.
- [31] Bentolila, L.A. and S. Weiss, "Single-step multicolor fluorescent in situ hybridization analysis using semiconductor quantum dot-DNA conjugates," *Cell Biochemistry and Biophysics*, 2006. 45(1): 59–70.
- [32] Chan, P., et al., "Method for multiplex cellular detection of mRNAs using quantum dot fluorescent in situ hybridization," *Nucleic Acids Res*, 2005. 33(18): e161.
- [33] Jaiswal, J.K., et al., "Long-term multiple color imaging of live cells using quantum dot bioconjugates," *Nature Biotechnol.*, 2003. 21(1): 47–51.
- [34] Mansson, A., et al., "In vitro sliding of actin filaments labelled with single quantum dots," *Biochem. Biophys. Res. Commun.*, 2004. 314(2): 529–34.
- [35] Marks, K.M., M. Rosinov, and G.P. Nolan, "In Vivo Targeting of Organic Calcium Sensors via Genetically Selected Peptides," *Chem. Biol.*, 2004. 11: 347–356.
- [36] Whaley, S.R., et al., "Selection of peptides with semiconductor binding specificity for directed nanocrystal assembly," *Nature*, 2000. 405(6787): 665–668.
- [37] Lee, S.-W., et al., "Ordering of Quantum Dots Using Genetically Engineered Viruses," *Sciences*, 2002. 296: 892–895.

- [38] Zhou, M. and I. Ghosh, "Quantum dots and peptides: a bright future together," *Peptide Science*, 2007. 88(3): 325–339.
- [39] Cobbett, C.S., "Heavy metal detoxification in plants: Phytochelatin biosynthesis and function," *Iubmb Life*, 2001. 51(3): 183–188.
- [40] Dameron, C.T., et al., "Biosynthesis of cadmium sulphide quantum semiconductor crystallites," *Nature*, 1989. 338: 596–597.
- [41] Dameron, C.T. and D.R. Winge, "Peptide-Mediated Formation of Quantum Semiconductors," *Trends in Biotechnology*, 1990. 8(1): 3–6.
- [42] Sukhanova, A., et al., "Highly Stable Fluorescent Nanocrystals as a Novel Class of Labels for Immunohistochemical Analysis of Paraffin-Embedded Tissue Sections," *Laboratory Investigation*, 2002. 82(9): 1259.
- [43] Bae, W. and R.K. Mehra, "Cysteine-capped ZnS nanocrystallites: Preparation and characterization," *Journal of Inorganic Biochemistry*, 1998. 70(2): 125–135.
- [44] Iyer, G., et al., "Solubilization of quantum dots with a recombinant peptide from *Escherichia coli*," *Small*, 2007. 3(5): 793–798.
- [45] Zheng, Y., S. Gao, and J.Y. Ying, "Synthesis and cell-imaging applications of glutathione-capped CdTe quantum dots," *Advanced Materials*, 2007. 19: 376–380.
- [46] Doose, S., et al., "Comparison of Photophysical and Colloidal Properties of Biocompatible Semiconductor Nanocrystals Using Fluorescence Correlation Spectroscopy," *PUB?* 2005.
- [47] Mao, C., et al., "Virus-based toolkit for the directed synthesis of magnetic and semiconducting nanowires," *Science*, 2004. 303(5655): 213–217.
- [48] Brown, S., "Engineered iron oxide-adhesion mutants of the *Escherichia coli* phage  $\phi$  receptor. Proc Natl Acad Sci USA, 1992. 89: 8651–8655.
- [49] Waggoner, A., "Covalent labeling of proteins and nucleic acids with fluorophores," *Methods in Enzymology*, 1995. 246(5): 362–73.
- [50] Hermanson, G., "Bioconjugate Techniques," *PUB?* 1996, San Diego, CA: Academic Press, Inc.
- [51] Pinaud, F., et al., "Advances in fluorescence imaging with quantum dot bio-probes," *Biomaterials*, 2005. 27(9): 1679–1687.
- [52] Saxton, M.J. and K. Jacobson, "Single-particle tracking: applications to membrane dynamics," *Annu. Rev. Biophys. Biomol. Struct.*, 1997. 26: 373–399.
- [53] Ueda, M., et al., "Single-molecule analysis of chemotactic signaling in *Dictyostelium* cells," *Science*, 2001. 294(5543): 864–867.
- [54] Tsay, J.M., et al., "Enhancing the photoluminescence of peptide-coated CdSe nanocrystals with shell composition and UV irradiation," *Journal of Physical Chemistry*, 2005.
- [55] Meier, J., et al., "Fast and reversible trapping of surface glycine receptors by gephyrin," *Nat. Neurosci.*, 2001. 4(3): 253–60.
- [56] Schmidt, T., et al., "Imaging of single molecule diffusion," *Proceedings of the National Academy of Sciences USA*, 1996. 93: 2926–2929.
- [57] Derfus, A.M., W.C.W. Chan, and S.N. Bhatia, "Intracellular delivery of quantum dots for live cell labeling and organelle tracking," *Adv. Mater.*, 2004. 16(12): 961–966.
- [58] Lagerholm, B.C., et al., "Multicolor Coding of Cells with Cationic Peptide Coated Quantum Dots," *Nano Letters*, 2004. 4(10): 2019–2022.
- [59] Silver, J. and W. Ou, "Photoactivation of quantum dot fluorescence following endocytosis," *Nano Lett*, 2005. 5(7): 1445–1449.
- [60] Chen, F. and D. Gerion, "Fluorescent CdSe/ZnS Nanocrystal-Peptide Conjugates for Long-term, Nontoxic Imaging and Nuclear Targeting in Living Cells," *Nano Letters*, 2004. 4(10): 1827–1832.
- [61] Wadia, J.S. and S.F. Dowdy, "Protein transduction technology," *Curr Opin Biotechnol*, 2002. 13(1): 52–56.

- [62] Anikeeva, N., et al., "Quantum dot/peptide-MHC biosensors reveal strong CD8-dependent cooperation between self and viral antigens that augment the T cell response," *Proc. Natl. Acad. Sci. USA*, 2006. 103(45): 16846–16851.
- [63] Cai, W., et al., "Peptide-Labeled Near-Infrared Quantum Dots for Imaging Tumor Vasculature in Living Subjects," *Nano Lett.*, 2006. 6(4): 669–676.
- [64] Kim, Y., et al., "Targeting Heat Shock Proteins on Cancer Cells: Selection, Characterization, and Cell-Penetrating Properties of a Peptidic GRP78 Ligand," *Biochemistry*, 2006. 45(31): 9434–9444.
- [65] Xue, F., et al., "Enhancement of intracellular delivery of CdTe quantum dots (QDs) to living cells by Tat conjugation," *Journal of Fluorescence*, 2007. 17(2): 149–154.
- [66] Zhou, M., et al., "Peptide-Labeled Quantum Dots for Imaging GPCRs in Whole Cells and as Single Molecules," *Bioconjugate Chem.*, 2007. 18(2): 323–332.
- [67] Delehanty, J.B., et al., "Self-Assembled Quantum Dot-Peptide Bioconjugates for Selective Intracellular Delivery," *Bioconjugate Chem.*, 2006. 17(4): 920–927.
- [68] Medintz, I.L., et al., "Designer Variable Repeat Length Polypeptides as Scaffolds for Surface Immobilization of Quantum Dots," *J. Phys. Chem. B*, 2006. 110(22): 10683–10690.
- [69] Vu, T.Q., et al., "Peptide-Conjugated Quantum Dots Activate Neuronal Receptors and Initiate Downstream Signaling of Neurite Growth," *Nano Lett.*, 2005. 5(4): 603–607.
- [70] Prochiantz, A., "Protein and peptide transduction, twenty years later a happy birthday," *Advanced Drug Delivery Reviews*, 2008. 60(4-5): 448–451.
- [71] Wender, P.A., et al., "The design, synthesis, and evaluation of molecules that enable or enhance cellular uptake: peptoid molecular transporters," *Proc. Natl. Acad. Sci. USA*, 2000. 97(24): 13003–13008.
- [72] Hoshino, A., et al., "Quantum dots targeted to the assigned organelle in living cells," *Microbiology and Immunology*, 2004. 48(12): 985–994.
- [73] Mattheakis, L.C., et al., "Optical coding of mammalian cells using semiconductor quantum dots," *Anal. Biochem.*, 2004. 327(2): 200–208.
- [74] Biju, V., et al., "Quantum dot-insect neuropeptide conjugates for fluorescence imaging, transfection, and nucleus targeting of living cells," *Langmuir*, 2007. 23(20): 10254–10261.
- [75] Gambhir, S.S., "Molecular imaging of cancer with positron emission tomography," *Nat. Rev. Cancer*, 2002. 2(9): 683–693.
- [76] Massoud, T.F. and S.S. Gambhir, "Molecular imaging in living subjects: seeing fundamental biological processes in a new light," *Genes Dev*, 2003. 17(5): 545–580.
- [77] Helmchen, F. and W. Denk, "Deep tissue two-photon microscopy," *Nature Methods*, 2005. 2(12): 932–940.
- [78] Schipper, M.L., et al., "microPET-based biodistribution of quantum dots in living mice," *J. Nucl. Med.*, 2007. 48(9): 1511–1518.
- [79] Cai, W., et al., "Dual-function probe for PET and near-infrared fluorescence imaging of tumor vasculature," *J. Nucl. Med.*, 2007. 48(11): 1862–1870.
- [80] Woodward, J.D., et al., "In vivo SPECT/CT imaging and biodistribution using radioactive Cd[125m]Te/ZnS nanoparticles," *Nanotechnology*, 2007. 18(17): 175103.1–175103.5.
- [81] Tromberg, B.J., et al., "Non-invasive in vivo characterization of breast tumors using photon migration spectroscopy," *Neoplasia*, 2000. 2(1-2): 26–40.
- [82] Rice, B.W., M.D. Cable, and M.B. Nelson, "In vivo imaging of light-emitting probes," *J. Biomed. Opt.*, 2001. 6(4): 432–440.
- [83] Weissleder, R., et al., "In vivo imaging of tumors with protease-activated near-infrared fluorescent probes," *Nat. Biotechnol.*, 1999. 17(4): 375–378.
- [84] Weissleder, R., "A clearer vision for in vivo imaging," *Nat. Biotechnol.*, 2001. 19(4): 316–317.
- [85] Frangioni, J.V., "In vivo near-infrared fluorescence imaging," *Curr. Opin. Chem. Biol.*, 2003. 7(5): 626–34.

- [86] Kim, S., et al., "Near-infrared fluorescent type II quantum dots for sentinel lymph node mapping," *Nature Biotechnol.*, 2004. 22(1): 93–97.
- [87] Ballou, B., et al., "Noninvasive imaging of quantum dots in mice," *Bioconjug. Chem.*, 2004. 15(1): 79–86.
- [88] Kirchner, C., et al., "Cytotoxicity of Colloidal CdSe and CdSe/ZnS Nanoparticles," *Nano Lett.*, 2005. 5(2): 331–338.
- [89] Derfus, A.M., W.C.W. Chan, and S.N. Bhatia, "Probing the Cytotoxicity of Semiconductor Quantum Dots," *Nano. Lett.*, 2004. 4(1): 11–18.
- [90] Giepmans, B.N., et al., "Correlated light and electron microscopic imaging of multiple endogenous proteins using Quantum dots," *Nature Methods*, 2005. 2(10): 743–749.
- [91] Shi, P., et al., "Peptide-Directed Binding of Quantum Dots to Integrins in Human Fibroblast," *IEEE Transactions on Nanobioscience*, 2006. 5(1): 15–19.
- [92] Lieleg, O., et al., "Specific integrin labeling in living cells using functionalized nanocrystals," *Small*, 2007. 3(9): 1560–1565.
- [93] Xiong, J.P., et al., "Crystal structure of the extracellular segment of integrin alpha Vbeta3 in complex with an Arg-Gly-Asp ligand," *Science*, 2002. 296(5565): 151–155.
- [94] Hood, J.D. and D.A. Cheresh, "Role of integrins in cell invasion and migration," *Nat. Rev. Cancer*, 2002. 2(2): 91–100.
- [95] Jin, H. and J. Varner, "Integrins: roles in cancer development and as treatment targets," *Br. J. Cancer*, 2004. 90(3): 561–565.
- [96] Chen, X., P.S. Conti, and R.A. Moats, "In vivo near-infrared fluorescence imaging of integrin alphavbeta3 in brain tumor xenografts," *Cancer Res.*, 2004. 64(21): 8009–8014.
- [97] Mammen, M., S.-K. Choi, and G.M. Whitesides, "Polyvalent Interactions in Biological Systems: Implications for Design and Use of Multivalent Ligands and Inhibitors," *Angew. Chem. Int. Ed.*, 1998. 37: 2754–2794.
- [98] Chen, X., et al., "Micro-PET imaging of alphavbeta3-integrin expression with 18F-labeled dimeric RGD peptide," *Mol. Imaging*, 2004. 3(2): 96–104.
- [99] Wu, Y., et al., "microPET imaging of glioma integrin {alpha}v{beta}3 expression using (64)Cu-labeled tetrameric RGD peptide," *J. Nucl. Med.*, 2005. 46(10): 1707–1718.
- [100] Richard, I., "The genetic and molecular bases of monogenic disorders affecting proteolytic systems," *J. Med. Genet.*, 2005. 42(7): 529–539.
- [101] Funovics, M., R. Weissleder, and C.H. Tung, "Protease sensors for bioimaging," *Anal. Bioanal. Chem.*, 2003. 377(6): 956–963.
- [102] Chang, E., et al., "Protease-activated quantum dot probes," *Biochem. Biophys. Res. Commun.*, 2005. 9(334): 1317–1321.
- [103] Medintz, I.L., et al., "Proteolytic activity monitored by fluorescence resonance energy transfer through quantum-dot-peptide conjugates," *Nature Material*, 2006. 5(7): 581–589.
- [104] Shi, L., et al., "Synthesis and application of quantum dots FRET-based protease sensors," *J. Am. Chem. Soc.*, 2006. 128(32): 10378–10379.
- [105] Dougherty, T.J., "Photosensitizers: therapy and detection of malignant tumors," *Photochemistry and Photobiology*, 1987. 45(6): 879–889.
- [106] Ochsner, M., "Photophysical and photobiological processes in the photodynamic therapy of tumours," *Journal of Photochemistry and Photobiology Biology*, 1997. 39(1): 1–18.
- [107] Bakalova, R., et al., "Quantum dots as photosensitizers?" *Nature Biotechnology*, 2004. 22(11): 1360–1361.
- [108] Samia, A.C., S. Dayal, and C. Burda, "Quantum dot-based energy transfer: perspectives and potential for applications in photodynamic therapy," *Photochemistry and Photobiology*, 2006. 82(3): 617–625.
- [109] Samia, A.C., X. Chen, and C. Burda, "Semiconductor quantum dots for photodynamic therapy," *Journal of the American Chemical Society*, 2003. 125(51): 15736–15737.

- [110] Hsieh, J.M., et al., "Iridium-complex modified CdSe/ZnS quantum dots; a conceptual design for bifunctionality toward imaging and photosensitization," *Chemical Communications*, 2006. 6: 615–617.
- [111] Shi, L., B. Hernandez, and M. Selke, "Singlet oxygen generation from water-soluble quantum dot organic dye nanocomposites," *Journal of the American Chemical Society*, 2006. 128(19): 6278–6279.
- [112] Tsay, J.M., et al., "Singlet Oxygen Production by Peptide-Coated Quantum Dot-Photosensitizer Conjugates," *J. Am. Chem. Soc.*, 2007. 129(21): 6865–6871.
- [113] Choi, H.S., et al., "Renal clearance of quantum dots," *Nature Biotechnology*, 2007. 25(10): 1165–1170.
- [114] Aharoni, A., et al., "Synthesis of InAs/CdSe/ZnSe core/shell1/shell2 structures with bright and stable near-infrared fluorescence," *J. Am. Chem. Soc.*, 2006. 128(1): 257–264.
- [115] Boder, E.T., K.S. Midelfort, and K.D. Wittrup, "Directed evolution of antibody fragments with monovalent femtomolar antigen-binding affinity," *Proc. Natl. Acad. Sci. USA*, 2000. 97(20): 10701–10705.
- [116] Zhang, Y., M.K. So, and J. Rao, "Protease-modulated cellular uptake of quantum dots," *Nano Letters*, 2006. 6(9): 1988–1992.